

PROCESS MODELING FOR DIMENSIONAL CONTROL – SENSITIVITY ANALYSIS OF A COMPOSITE SPAR PROCESS

Göran Fernlund¹, Anoush Poursartip¹, Karl Nelson², Mark Wilenski², Frederick Swanstrom³

¹Metals and Materials Engineering, The University of British Columbia, Vancouver, Canada

²Boeing Phantom Works, Seattle, USA, ³Manufacturing Engineering, Boeing Composites
Manufacturing Center, Frederickson, USA

ABSTRACT

Dimensional fidelity and dimensional control of composite parts are important for cost effective assembly of large composite structures, and are essential for concepts such as shim-less assembly. There has been considerable work to take a more science-based approach to the understanding and the prediction of the autoclave process through computer simulations. This paper discusses current capabilities and future challenges of finite element based modeling of the autoclave process, with a focus on residual stress build-up and its impact on dimensional fidelity. Specifically, the predictive capabilities of the finite element based software “COMPRO” are illustrated through a case study where the sensitivity of a composite front spar process is analyzed. Model predictions of flange spring-in are compared to measurements on manufactured pre-production spars, and suggestions for future model improvements proposed.

KEY WORDS: Process Modelling, Dimensional Control, Warpage

1. INTRODUCTION

Computer simulations of manufacturing processes are gaining ground in industry because of increased understanding of fundamental phenomena and the availability of computing resources, leading to increasing accuracy of model predictions. Several models have been developed for the simulation of processing of polymeric composite materials [e.g. 1-9]. Most models presented in the literature were developed with a focus on the fundamental science rather than for the purpose of simulation of processes in an industrial setting. “COMPRO” [10-13], on the other hand, is a finite element based composites process model that was developed for the simulation of autoclave processing in an industrial setting. The software was developed by the Composites Group at the University of British Columbia with substantial input from The Boeing Company to ensure that it includes industrially relevant effects.

For the past three years, the UBC Composites Group has worked closely with the Boeing Commercial Airplane Group and Boeing Phantom Works in applying COMPRO to industrial parts and processes. The work has involved detailed characterization of Boeing materials systems for processing purposes, and the analysis of existing and new processes and parts on Boeing 747, 767, and 777 airplanes.

2. COMPOSITE FRONT SPAR PROCESS

2.1 Problem description The front spar that is analyzed is best described as a carbon/epoxy C-channel with varying left and right flange angles to accommodate the airfoil shape. The dimensional control of the flange angles of the front spar is critical to obtain an aerodynamically correct leading edge profile. Both flanges have a toggle approximately halfway down the flange to accommodate the difference in thickness between the leading edge and the wing skin, see Figure 1.

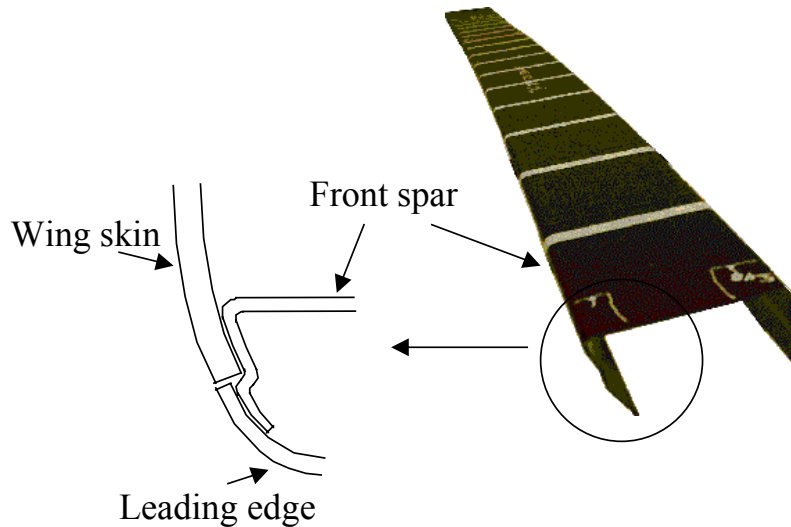


Figure 1. Photograph of a pre-production spar (right), and a schematic of the front spar attachment to the wing skin and the leading edge (left).

2.2 Typical deformation Experience has shown that autoclave moulded C-channels made on a convex (male) tool typically exhibit three types of process induced deformations: (1) flange spring-in, (2) web warpage away from the tool, and (3) corner thinning, see Figure 2. The magnitude of the deformations, especially due to flange spring-in, is often large enough that they have to be compensated for in tool design. The amount of deformation for a given part and process is dependent on a number of process parameters, and is analyzed through computer simulations in this study.

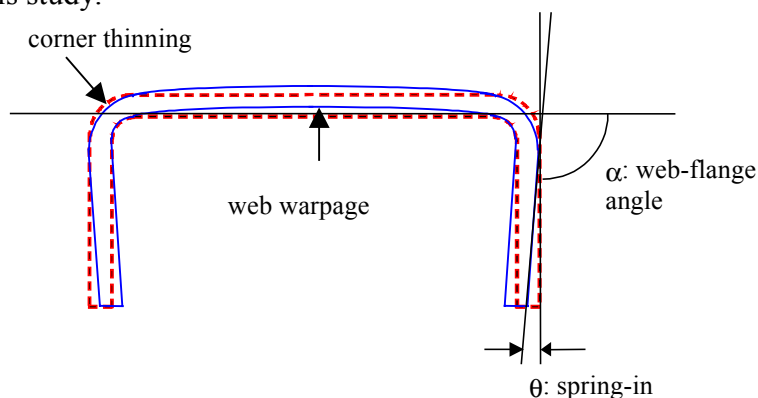


Figure 2. Schematic of typical process induced deformations of an autoclave molded C-channel made on a convex (male) tool (dashed line: initial shape, solid line: shape after processing).

3. SENSITIVITY ANALYSIS

COMPRO is a 2-D FEM model and a structure such as the front spar shown in Figure 1 is analyzed by modelling representative cross-sections of it. In the present case, two cross-sections are analyzed, one at the root end and one at the tip end of the spar. Using COMPRO, process models are developed and a virtual designed experiment that evaluates the effect of changes in various process parameters (factors) on the predicted process induced deformations (response) is performed. A designed experiment not only gives information about the effect of individual factors but also the effect of interactions between them. The knowledge gained can be used to aid in tool design, detailed part design, choice of materials, and the development of an appropriate cure cycle for the process. Although the focus in the current study is the process induced deformations, COMPRO provides a wealth of information about the process: temperature, degree of cure, and stress build-up in the part throughout the cure cycle.

Table 1 shows a list of parameters that are used in the present sensitivity analysis. The parameters are divided into process related and model related parameters, which are studied separately, to keep the size of the designed experiment small. The selection of parameters and their levels are based on factory experience and previous modelling work on similar parts and processes.

Table 1. Process and model related parameters used in the sensitivity analysis.

Process related parameters	Description	Hi/Low levels
X ₁	cross-section	12 ply section / 6 ply section
X ₂	laid up flange length	2.75"/2.25"
X ₃	tool thermal mass	solid core/hollow core
X ₄	heat-up rate	5/1 (°F/min)
X ₅	toggle radius	high/low (nominal / +25%)
Model related parameters	Description	Hi/Low levels
X ₆	cure kinetics	+/-10% of nominal*
X ₇	modulus development	+/-10% of nominal*
X ₈	resin CTE	+/-10% of nominal*
X ₉	resin cure shrinkage	+/-10% of nominal*
X ₁₀	resin viscosity	+/-10% of nominal*

**The nominal values of the model related parameters are based on extensive materials characterization for the Hexcel F593/AS4 (BMS8-256) prepreg system.*

Two "Resolution V" (2_v^{5-1}) fractional factorial experiments [14] were performed to determine the sensitivity of the COMPRO predictions of flange spring-in and web warpage (see Figure 2) to variations in process related and model related parameters, respectively. Spring-in angles were determined from the model predictions by fitting lines to two points on each segment on the tool-side of the part. The spring-in was defined as the difference between the final and initial angles between line segments, and was determined for each of the four major angles shown in Figure 3. The web warpage, δ , was characterized by the vertical displacement away from the tool of the center of the web from a straight line joining points near its edges.

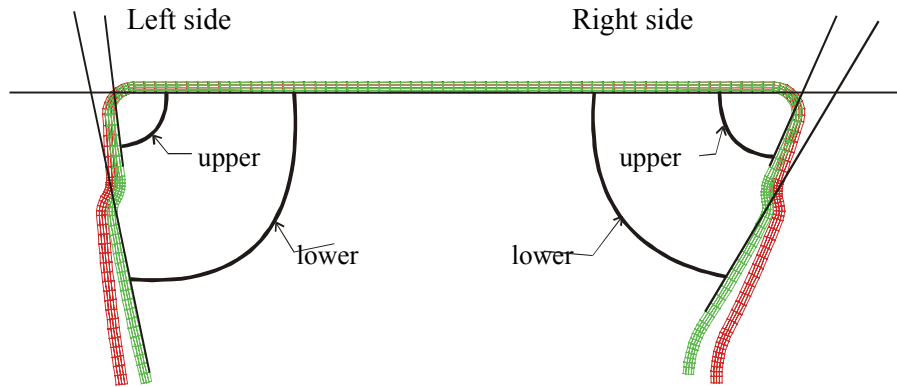


Figure 3. Original and deformed finite element meshes (geometries) of the front spar illustrating the definition of spring-in angles.

3.1 Description of process related parameters

3.1.1 Cross-section (X_1) Two cross-sections of the front spar were modeled. One close to the wing tip (“tip”) and the second near the root of the wing (“root”), see Figure 4.

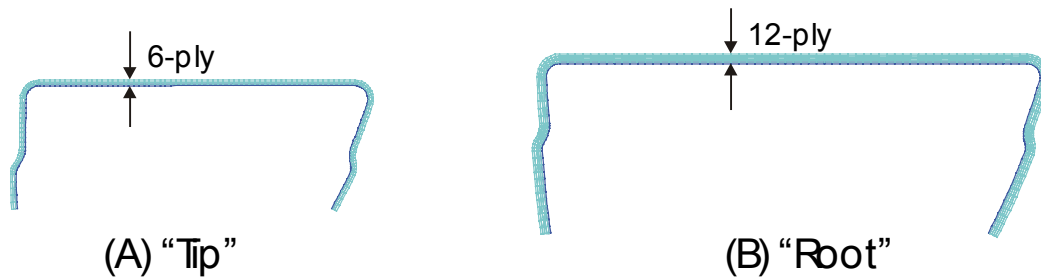


Figure 4. Modeled cross-sections of the front spar a) near tip and b) near root. Note that only the finite element mesh of the part is shown, and that the meshes are to scale relative to each other.

3.1.2 Laid-up flange length (X_2) The high and low settings for the flange length were 2.75” (nominal) and 2.25” respectively (Figure 5).

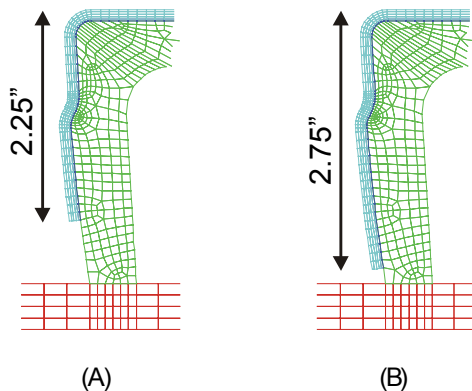


Figure 5. Flange length a) “Low” setting and b) “High” setting (nominal).

3.1.3 Tool thermal mass (X_3) The tool is made of Invar, and two tooling concepts were modeled. The “High” setting represents a tool with a solid core and the “Low” setting represents a tool with a hollow core. The hollow core tool has a wall thickness of approximately 0.5 inches (Figure 6).

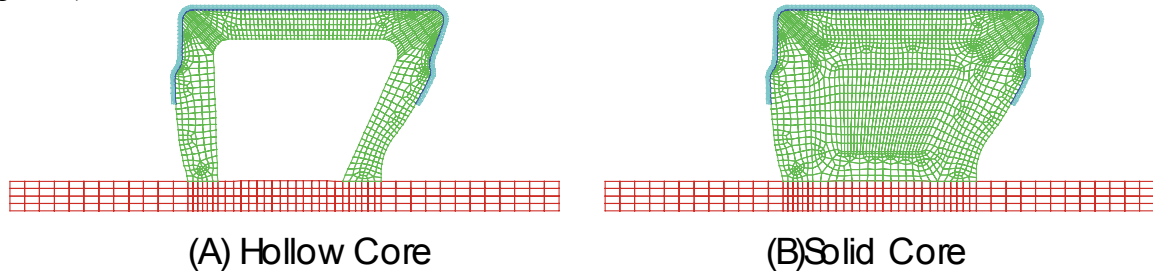


Figure 6. Tool thermal mass a) “Low” setting and b) “High” setting.

3.1.4 Heat-up Rate (X_4) The standard cure cycle is a single-hold cycle with a 140-minute hold. The “High” and “Low” settings for the heat-up rate parameter were 5°F/min and 1°F/min, respectively. The cool-down rate was fixed at 4.25 °F/min and the autoclave pressure and bag pressure were 92.5 and 0 psig., respectively.

3.1.5 Toggle radius (X_5) The actual (nominal) toggle radii were used as the “Low” setting for this parameter. The “High” value for this parameter was 25% greater (Figure 7).

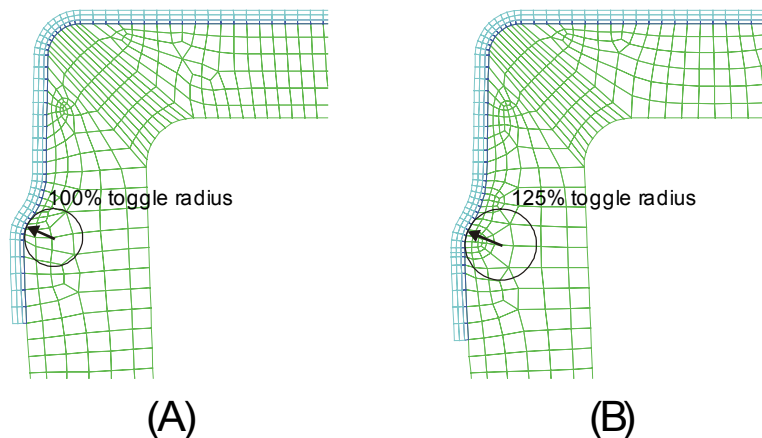


Figure 7. Example toggle radii a) “Low” setting and b) “High” setting.

3.2 Description of model related parameters Model material parameters for resin cure kinetics, modulus development, CTE, cure shrinkage, and resin viscosity were varied to high and low settings. The range of these settings was such that it encompassed the range of experimental values upon which the original setting was based. All model related parameters are described with analytical functions that are dependent on the degree of cure and temperature in COMPRO. The form of the equations used and the value of various constants in them are dependent on the prepreg system, BMS8-256, a carbon fabric/epoxy 350°F curing system.

3.3 Experimental Design A “Resolution V” (2_v^{5-1}) experimental design [14] was used to determine the effect of the process and model related parameters on the COMPRO model response (Table 2). Sixteen COMPRO runs were performed for each group of parameters,

allowing for the analysis of both single-factor effects and two-factor interactions within each group. Table 3 shows the experimental design for the model related parameters.

Table 2. Resolution V (2_v^{5-1}) experimental design for the process related parameters (+ indicates the “High” setting, and - the “Low” setting).

Run	X ₁ : Cross-section	X ₂ : Toggle Radius	X ₃ : Flange Length	X ₄ : Tool Thermal Mass	X ₅ : Heating Rate
DOE-1	-	-	-	-	+
DOE-2	+	-	-	-	-
DOE-3	-	+	-	-	-
DOE-4	+	+	-	-	+
DOE-5	-	-	+	-	-
DOE-6	+	-	+	-	+
DOE-7	-	+	+	-	+
DOE-8	+	+	+	-	-
DOE-9	-	-	-	+	-
DOE-10	+	-	-	+	+
DOE-11	-	+	-	+	+
DOE-12	+	+	-	+	-
DOE-13	-	-	+	+	+
DOE-14	+	-	+	+	-
DOE-15	-	+	+	+	-
DOE-16	+	+	+	+	+

Table 3. Resolution V (2_v^{5-1}) experimental design for the model related parameters (+ indicates the “High” setting, and - the “Low” setting).

Run	X ₆ : Cure Kinetics	X ₇ : Modulus Development	X ₈ : Resin CTE	X ₉ : Cure Shrinkage	X ₁₀ : Resin Viscosity
DOE-17	-	-	-	-	+
DOE-18	+	-	-	-	-
DOE-19	-	+	-	-	-
DOE-20	+	+	-	-	+
DOE-21	-	-	+	-	-
DOE-22	+	-	+	-	+
DOE-23	-	+	+	-	+
DOE-24	+	+	+	-	-
DOE-25	-	-	-	+	-
DOE-26	+	-	-	+	+
DOE-27	-	+	-	+	+
DOE-28	+	+	-	+	-
DOE-29	-	-	+	+	+
DOE-30	+	-	+	+	-
DOE-31	-	+	+	+	-
DOE-32	+	+	+	+	+

3.4 Results - Process related parameters The results of the sixteen COMPRO runs for the process related parameters were analyzed to determine the effect on two model responses: flange spring-in and web warpage, see Figure 2 and Figure 3. Corner thinning was not significant in the present case. Table 4 shows the predicted flange spring-in and web-warpage for the 16 runs in the designed experiment for the process related parameters.

Table 4. Predicted spring-in angles and web warpage for the process related parameters. (For definitions, see Figure 2 and Figure 3)

Run #	Flange Spring-in Angle (degrees)				Web Warpage (mils)
	Lower-left	Upper-left	Lower-right	Upper-right	
DOE-1	1.43	1.44	1.77	1.75	1.13
DOE-2	1.43	1.39	1.66	1.59	3.01
DOE-3	1.44	1.45	1.78	1.76	0.85
DOE-4	1.44	1.40	1.67	1.60	2.55
DOE-5	1.47	1.45	1.82	1.76	0.88
DOE-6	1.46	1.39	1.67	1.60	2.65
DOE-7	1.46	1.44	1.82	1.75	0.86
DOE-8	1.47	1.40	1.68	1.60	2.57
DOE-9	1.45	1.46	1.79	1.77	0.90
DOE-10	1.46	1.42	1.69	1.62	2.77
DOE-11	1.45	1.46	1.79	1.77	0.92
DOE-12	1.46	1.42	1.70	1.62	2.63
DOE-13	1.48	1.46	1.84	1.78	0.95
DOE-14	1.48	1.42	1.69	1.63	2.68
DOE-15	1.48	1.45	1.84	1.77	0.84
DOE-16	1.49	1.42	1.70	1.63	2.75

By performing an analysis of the COMPRO results above, the main effect of each factor (X_i) and all first-order interaction effects on the response (Y) were determined. The response equation, $Y=f(X_i)$, for a designed experiment can in general be written [14]

$$Y = \text{mean response} + \frac{1}{2}(C_1 * X_1 + C_2 * X_2 + \dots C_{12} * X_1 * X_2 + \dots) \quad (1)$$

where C_{ij} represents the importance of the factors and combination of factors on the response, and X_i is the coded level for parameter i , either +1 or -1, representing the high and the low setting for that parameter, respectively. For an experimental design with sixteen runs, eq. (1) has sixteen terms that fully characterizes the response matrix in Table 4. In most cases, however, the response can be described to within a few percent with only a few terms. The coefficients, C_{ij} were determined from the results in Table 4, using standard techniques [14]. The following tables show the coefficients C_{ij} .

Table 5. Summary of the single factor effects (coefficients C_i in eq. 1) on spring-in and warpage.

Angle	Mean response (degrees)	C_1 : Cross Section (degrees)	C_2 : Toggle Radius (degrees)	C_3 : Flange Length (degrees)	C_4 : Tool Thermal Mass (degrees)	C_5 : Heating Rate (degrees)
Lower-Left	1.46	0.00	0.00	0.03	0.02	0.00
Upper-Left	1.43	-0.05	0.00	0.00	0.02	0.00
Lower-Right	1.74	-0.12	0.01	0.03	0.02	0.00
Upper-Right	1.69	-0.15	0.00	0.00	0.02	0.00
Warpage	(mils)	(mils)	(mils)	(mils)	(mils)	(mils)
δ (mils)	1.81	1.79	-0.13	-0.07	-0.01"	0.03"

Table 6. Summary of the of two-factor interaction effects (coefficients C_{ij} in eq. 1) on spring-in and warpage.

Angle	C_{12}	C_{13}	C_{14}	C_{15}	C_{23}	C_{24}	C_{25}	C_{34}	C_{35}	C_{45}
Lower-Left	0.00	0.00	0.00	0.00	0.00	0.00	0.00	0.00	0.00	0.00
Upper-Left	0.00	0.00	0.01	0.00	0.00	0.00	0.00	0.00	0.00	0.00
Lower-Right	0.00	-0.02	0.00	0.00	0.00	0.00	0.00	0.00	0.00	0.00
Upper-Right	0.00	0.00	0.00	0.00	-0.00	-0.00	0.00	0.00	0.00	0.00
Warpage										
δ (mils)	-0.03	-0.01	0.02	-0.07	0.09	0.08	0.02	0.07	0.03	0.06

If factors that have less than five percent effect on the response are omitted, the flange spring-in, θ , and the web warpage, δ , can be expressed using eq. (1), Table 5, and Table 6 as follows:

$$\theta_{Left}^{Lower} = 1.46^\circ \tag{2}$$

$$\theta_{Right}^{Lower} = 1.74^\circ - 0.06X_1 \tag{3}$$

$$\theta_{Left}^{Upper} = 1.43^\circ \tag{4}$$

$$\theta_{Right}^{Upper} = 1.69^\circ - 0.08X_1 \tag{5}$$

$$\delta = 1.81 + 0.90X_1 - 0.06X_2 + 0.04X_2X_3 \text{ (mils)} \tag{6}$$

Equations (2) – (5) predict the calculated spring-in in Table 4 to within 3%, and eq. (6) the web warpage to within 12.5%. Thus, of the studied process related parameters, the only one with an effect on spring-in greater than 5% is: X_1 :Cross-section. Of the studied process related parameters, the ones with the greatest effect (>5%) on web warpage are: X_1 : Cross-section , X_2 : Toggle Radius, and X_2X_3 : Toggle Radius/Flange Length.

3.5 Results - Model related parameters Table 7 shows a summary of the predicted spring-in and web-warpage for the 16 runs in the experimental design for the model related parameters (Table 3).

Table 7. Summary of predicted spring-in angles and web warpage for the model related parameters. (For definitions, see Figure 2 and Figure 3)

Run #	Flange Spring-in Angle (degrees)				Web Warpage (mils)
	Lower-left	Upper-left	Lower-right	Upper-right	
DOE-17	1.47	1.35	1.71	1.54	2.01
DOE-18	1.49	1.36	1.73	1.56	2.21
DOE-19	1.27	1.23	1.52	1.43	-1.65
DOE-20	1.37	1.32	1.64	1.54	-1.77
DOE-21	1.42	1.30	1.64	1.48	2.06
DOE-22	1.50	1.38	1.74	1.57	2.14
DOE-23	1.27	1.23	1.52	1.44	-1.70
DOE-24	1.38	1.32	1.64	1.55	-1.81
DOE-25	1.49	1.36	1.73	1.55	2.53
DOE-26	1.60	1.45	1.85	1.66	2.65
DOE-27	1.52	1.46	1.82	1.70	-1.88
DOE-28	1.65	1.58	1.96	1.84	-2.05
DOE-29	1.51	1.37	1.74	1.56	2.47
DOE-30	1.62	1.47	1.87	1.67	2.59
DOE-31	1.53	1.46	1.82	1.71	-1.91
DOE-32	1.65	1.58	1.97	1.84	-2.10

The coefficients C_{ij} in the response equations for the model related parameters were determined using the same technique as described earlier, and are shown in Table 8 and Table 9.

Table 8. Summary of the single factor effects (coefficients C_i in eq. 1) for spring-in and warpage.

Angle	Mean response (degrees)	C_6 : Cure Kinetics (degrees)	C_7 : Modulus Development (degrees)	C_8 : Resin CTE (degrees)	C_9 : Cure Shrinkage (degrees)	C_{10} : Resin Viscosity (degrees)
Lower-Left	1.48	0.10	-0.06	0.00	0.17	0.01
Upper-Left	1.39	0.09	0.02	0.00	0.15	0.01
Lower-Right	1.74	0.11	-0.02	0.00	0.20	0.01
Upper-Right	1.60	0.10	0.06	0.00	0.18	0.01
Warpage	(mils)	(mils)	(mils)	(mils)	(mils)	(mils)
δ (mils)	0.25	-0.03	-4.22	-0.06	0.08	0.01

Table 9. Summary of the of two-factor interaction effects (coefficients C_{ij} in eq. 1) for spring-in and warpage.

Angle	C_{67}	C_{68}	C_{69}	C_{610}	C_{78}	C_{79}	C_{710}	C_{89}	C_{810}	C_{910}
Lower-Left	0.02	0.01	0.02	-0.01	0.00	0.09	-0.01	0.01	-0.01	-0.01
Upper-Left	0.02	0.01	0.02	-0.01	0.00	0.11	-0.01	0.01	-0.01	-0.01
Lower-Right	0.02	0.01	0.02	-0.01	0.00	0.09	-0.01	0.01	-0.01	-0.01
Upper-Right	0.02	0.01	0.02	-0.01	0.00	0.10	-0.01	0.01	-0.01	-0.01
Warpage										
δ (mils)	-0.12	0.01	0.00	-0.01	0.02	-0.33	-0.01	0.01	-0.03	-0.01

If factors that have less than five percent effect on the response are omitted, the flange spring-in, θ , and the web warpage, δ , can be expressed using eq. (1), Table 8, and Table 9 as follows:

$$\theta_{Left}^{Lower} = 1.48^\circ + 0.05X_6 + 0.09X_9 + 0.05X_7X_9 \quad (7)$$

$$\theta_{Right}^{Lower} = 1.74^\circ + 0.06X_6 + 0.10X_9 + 0.06X_7X_9 \quad (8)$$

$$\theta_{Left}^{Upper} = 1.39^\circ + 0.04X_6 + 0.08X_9 + 0.04X_7X_9 \quad (9)$$

$$\theta_{Right}^{Upper} = 1.60^\circ + 0.05X_6 + 0.09X_9 + 0.05X_7X_9 \quad (10)$$

$$\delta = 0.25 - 0.02X_6 - 2.11X_7 - 0.03X_8 + 0.04X_9 - 0.06X_6X_7 + 0.01X_7X_8 - 0.17X_7X_9 - 0.02X_8X_{10} \text{ (mils)} \quad (11)$$

Equations (7-9) predict the calculated spring-in in Table 7 to within 6%, and eq. (11) the web warpage to within 8%. Thus, of the studied process related parameters, the ones with the greatest effect (>5%) on spring-in are: X_9 : Resin cure shrinkage, X_6 : Resin cure kinetics, and X_7X_9 : Modulus development/Resin cure shrinkage. The mean values of the spring-in are slightly different in equations (7-10) compared to equations (2-5) because of different baseline settings.

The most significant parameters (>5%), for web warpage are: X_7 : Resin modulus development, X_7X_9 : Modulus development/Resin cure shrinkage, X_7X_6 : Modulus development/Resin cure kinetics, and X_6 : Resin cure kinetics

3.6 Comments on the results The sensitivity analysis shows that the spring-in of the right flange is greater than for the left flange, and that the spring-in is greater for the lower than for the upper flange on both sides. These results agree with experience that says that the spring-in, θ , should be proportional to web-flange angle, α , ($\theta = C \cdot \alpha$) (Figure 2).

The analysis also shows that of the studied process related parameters, the only one of significance is the cross-section, X_l . It should be noted that both the geometry and the lay-up are changed when this parameter is varied between its high and low setting (Figure 4).

Of the model related parameters, resin cure shrinkage, resin cure kinetics, and the interaction of modulus development and resin cure had the greatest effect on spring-in. In general, the model related parameters had a greater effect on the spring-in than the process related parameters.

4. COMPARISON OF MEASURED AND PREDICTED SPRING-IN OF THE FRONT SPAR

Using the response equations from the sensitivity analysis above, we can easily determine the predicted spring-in for the four angles at the tip and the root end of the spar in the nominal case. Figure 8 shows a plot of the predicted flange spring-in as a function of the web-flange angle, α . The figure clearly shows how the predicted spring-in, θ , is linearly dependent on the web-flange angle, α .

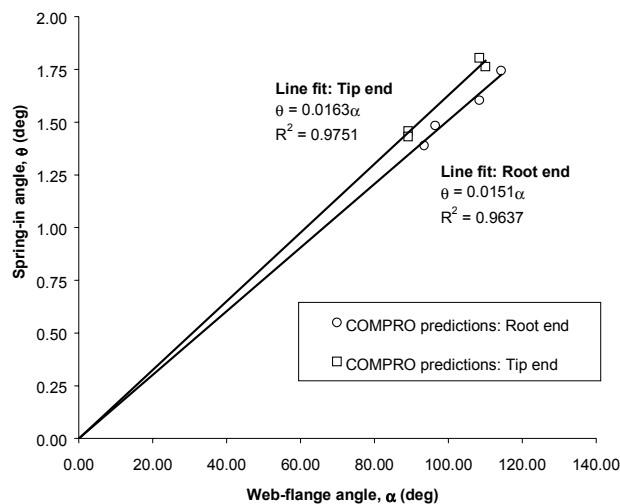


Figure 8. Predicted spring-in, θ , versus web-flange angle, α , and line fits to the data sets at both cross-sections.

The lay-up and the number of plies are different at the two cross-sections (root and tip) giving different slopes, C , of the fitted lines. The COMPRO predictions in Figure 8 suggest that the coefficient C in the equation above should be 0.0163 and 0.0151 for the tip and the root end, respectively. If one line is fitted to both data sets, the slope is 0.0157.

4.1 Experimental Data A full-scale spar was manufactured and the spring-in angles were calculated from measurements taken using a laser guided “Smart 310” tracking ball measurement system. Figure 9 shows the measured spring-in angles plotted against the web-flange angles. The data has a large amount of noise because of surface roughness on the bag side of the part where measurements were taken, and the small size of the flanges. If straight lines that are

forced to go through the origin are fitted to the data, the slopes of these lines are similar to those of the COMPRO predictions in Figure 8. The average value of the four slopes in Figure 9 is 0.0176, which is very close to the slope found for the COMPRO predictions above.

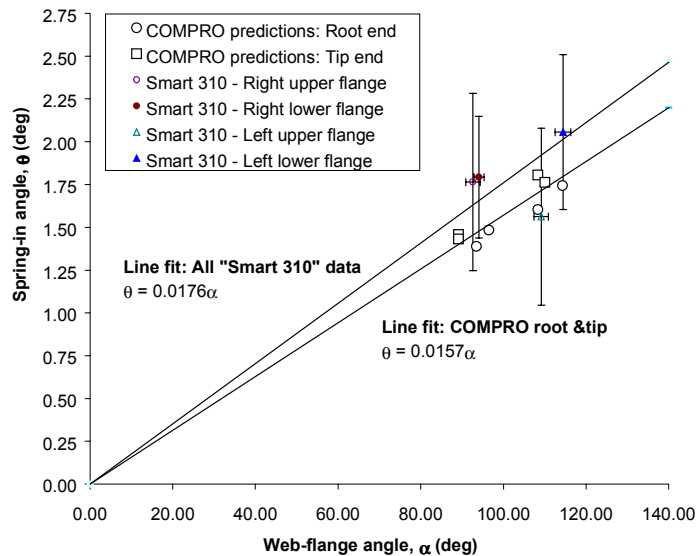


Figure 9. 'Smart-310' data presented as spring-in angles versus web-flange angle (alpha), and best line fits to each data set.

5. CONCLUSIONS

The case study shows that a composites process model can provide good predictions of process induced deformations for a simple solid laminate structure such as the front spar. However, there are currently many structures and processing issues of interest that are beyond the capabilities of a code such as COMPRO. Structures that are truly 3-D cannot be modeled with the current 2-D formulation. Other process problems of interest, such as core crush in honeycomb structures, cannot be modeled because of a lack of physical understanding of the problem. However, computer simulation of composites processing is becoming increasingly useful. With increasing knowledge and computer power, process modelling will one day become as common in the composites processing industry as it is in the plastics industry today.

6. ACKNOWLEDGEMENTS

We would like to thank United States Air Force Research Laboratory, Materials & Manufacturing Technology Directorate, Wright Patterson Air Force Base, Ohio, USA, for funding for the work, and our contract manager Dr. John D. Russell for his effort in leading and coordinating the "Processing for Dimensional Control" project (US Air Force contract #: F33615-97-C-5006).

7. REFERENCES

1. A.C. Loos and G.S. Springer, Curing of Epoxy Matrix, *J. of Composite Materials*, **17**, 2, 135-169 (1983).
2. R. Davé, J.L. Kardos and M.P. Dudukovic, Process Modeling of Thermosetting Matrix Composites: A Guide for Autoclave Cure Cycle Selection, *Proceedings of the American Society for Composites, 1st Technical Conference*, 137-153 (1986).

3. A.R. Mallow, F.R. Muncaster and F.C. Campbell, Science Based Cure Model for Composites, *Proceedings of the American Society for Composites, Third Technical Conference*, 171-186 (1986).
4. J. Mijovic and J. Wijaya, Effects of Graphite Fiber and Epoxy Matrix Physical Properties on the Temperature Profile Inside Their Composite During Cure, *SAMPE Journal*, **25**, **2**, 35-39 (1989).
5. T.A. Bogetti and J.W. Gillespie Jr., Process-Induced Stress and Deformation in Thick-Section Thermoset Composite Laminates, *J. of Composite Materials*, **26**, **5**, 626-660 (1992).
6. T.A. Bogetti and J.W. Gillespie Jr., Two-Dimensional Cure Simulation of Thick Thermosetting Composites, *J. of Composite Materials*, **25**, **3**, 239-273 (1991).
7. J.M. Kenny, Integration of Process Models with Control and Optimization of Polymer Composites Fabrication, *Proceedings of the Third Conference on Computer Aided Design in Composite Materials Technology*, 530-544 (1992).
8. S.R. White and H.T. Hahn, Process Modeling of Composite Materials: Residual Stress Development during Cure. Part I. Model Formulation, *J. of Composite Materials*, **26**, **16**, 2402-2422 (1992).
9. H.T. Hahn and N.J. Pagano, Curing Stresses in Composite Laminates, *J. of Composite Materials*, **9**, 91-108 (1975).
10. P. Hubert, "Aspects of flow and compaction of laminated composite shapes during cure", Ph.D. thesis, The University of British Columbia, Vancouver, Canada (1996).
11. A. J. Johnston, "An integrated model of the development of process-induced deformation in autoclave processing of composite structures", Ph.D. thesis, The University of British Columbia, Vancouver, Canada (1997).
12. P. Hubert, R. Vaziri, and A. Poursartip "A Two Dimensional Flow Model for the Process Simulation of Complex Shape Composite Laminates", to appear in *International Journal of Numerical Methods in Engineering* (1998).
13. J. Johnston, R. Vaziri, and A. Poursartip "A plane strain model for process-induced residual deformation of complex shaped composite laminates", paper submitted to *Journal of Composite Materials* (1998).
14. G.E.P. Box, W.G. Hunter, and J.S. Hunter, Statistics for experimenters: an introduction to design, data analysis, and model building, New York, Wiley (1978).